

## Supplementary Information

### CVD-Grown Monolayer MoS<sub>2</sub> in Bioabsorbable Electronics and Biosensors

Xiang Chen<sup>1†</sup>, Yong Ju Park<sup>1†</sup>, Minpyo Kang<sup>1†</sup>, Seung-Kyun Kang<sup>2</sup>, Jahyun Koo<sup>2</sup>, Sachin M. Shinde<sup>1</sup>, Jiho Shin<sup>2</sup>, Seunghyun Jeon<sup>3</sup>, Gayoung Park<sup>3</sup>, Ying Yan<sup>4</sup>, Matthew R. MacEwan<sup>4</sup>, Wilson Z. Ray<sup>4</sup>, Kyung-Mi Lee<sup>3\*</sup>, John A Rogers<sup>2\*</sup> & Jong-Hyun Ahn<sup>1\*</sup>

<sup>1</sup> School of Electrical and Electronic Engineering, Yonsei University, 50 Yonsei-ro, Seoul 03722, Republic of Korea

<sup>2</sup> Departments of Materials Science and Engineering, Biomedical Engineering, Chemistry, Mechanical Engineering, Electrical Engineering and Computer Science, Center for Bio-Integrated Electronics, Simpson Querrey Institute for Nano/Biotechnology, Northwestern University, Evanston, Illinois 60208, USA.

<sup>3</sup> Department of Biomedical Engineering, College of Health Science, Korea University, Seoul 136-703, Republic of Korea

<sup>4</sup> Department of Neurological Surgery, Washington University School of Medicine, St Louis, Missouri 63110, USA

<sup>†</sup>These authors contributed equally to this work.

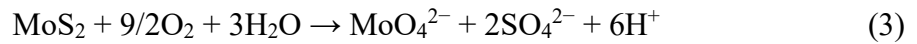
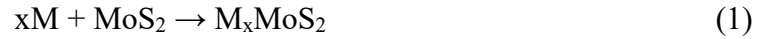
\*Corresponding authors:

kyunglee@korea.ac.kr, jrogers@northwestern.edu and ahnj@yonsei.ac.kr

## Supplementary Notes

### Supplementary Note 1. The possible reactions during MoS<sub>2</sub> biodegradation process in PBS solution

Since the dissolution tests of monolayer MoS<sub>2</sub> in this work involved PBS solution, which contains disodium hydrogen phosphate (Na<sub>2</sub>HPO<sub>4</sub>), sodium chloride (NaCl), potassium chloride (KCl), potassium dihydrogen phosphate (KH<sub>2</sub>PO<sub>4</sub>), O<sub>2</sub>, and H<sub>2</sub>O, likely reactions are<sup>1,2</sup>:



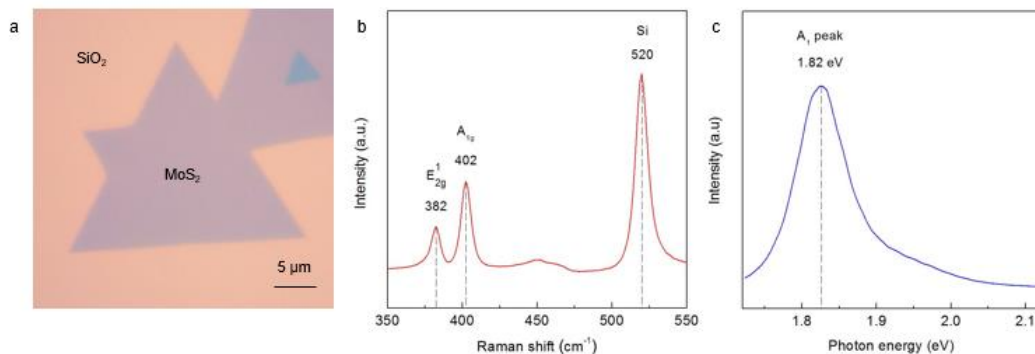
Where M = Na or K.

Besides, the empirical kinetic equation affected by pH level in PBS solution is<sup>3</sup>:

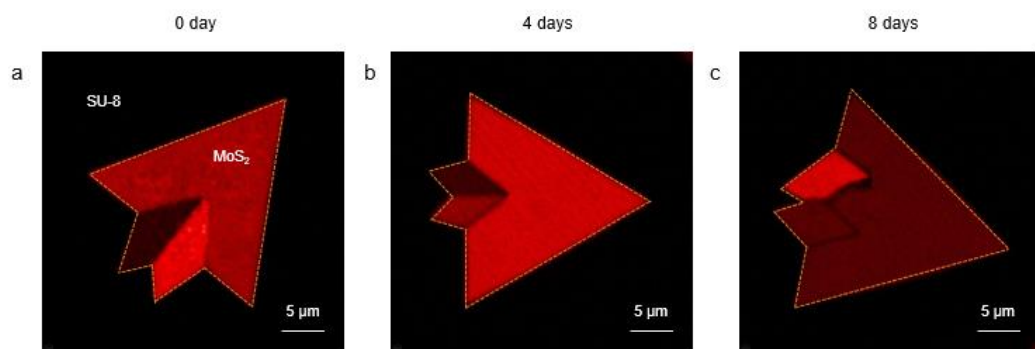
$$d[MoS_2]/[MoS_2]dt = 1.9*[OH^-]^{0.17}, 1/d \quad (4)$$

where the units of the dissolution rate and OH<sup>-1</sup> concentration are days<sup>-1</sup> and mol/L, respectively.

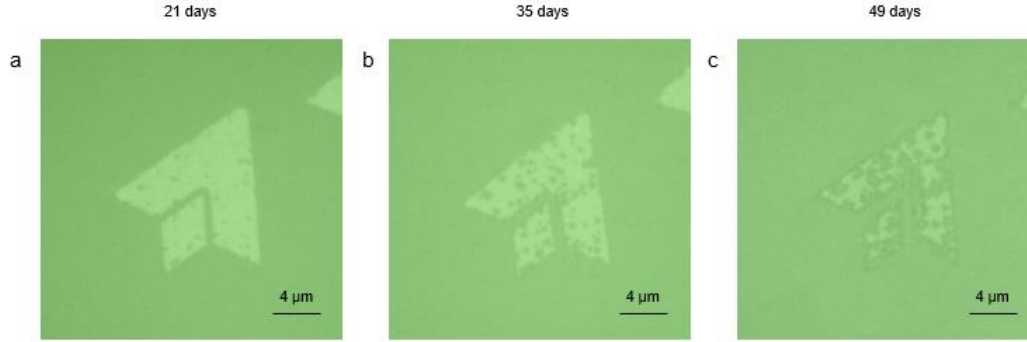
## Supplementary Figures



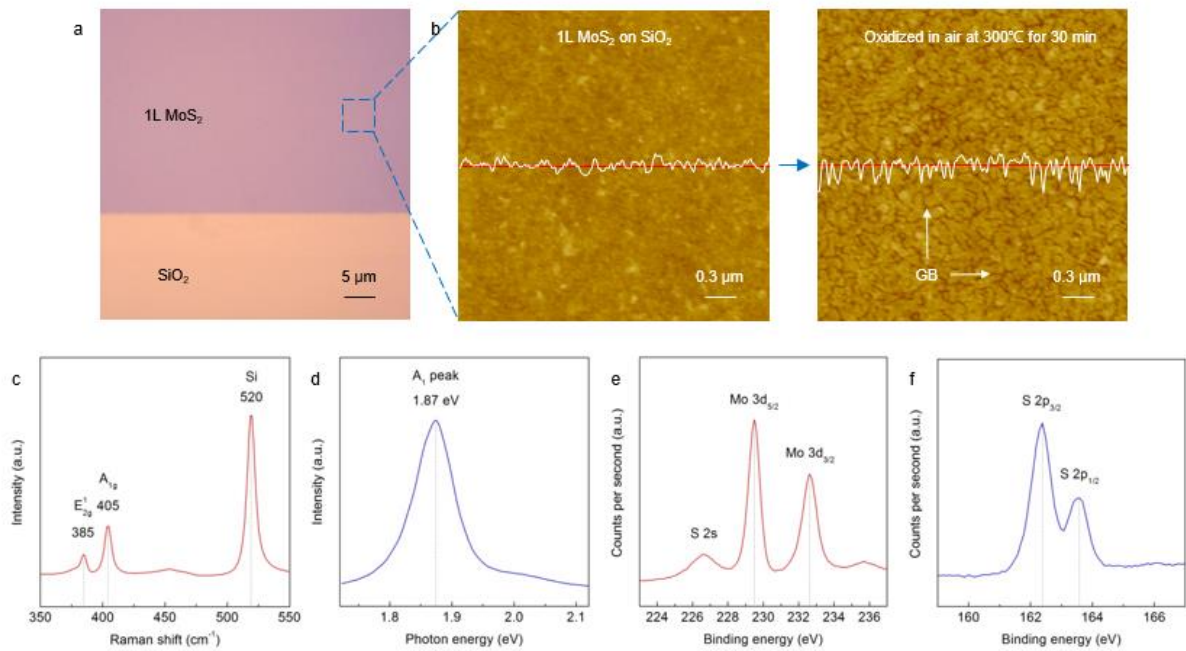
**Supplementary Figure 1 | The optical characterization of as-grown monolayer MoS<sub>2</sub> crystals.** **a**, OM image of isolated polycrystalline MoS<sub>2</sub> monolayer fabricated on SiO<sub>2</sub> substrate by using APCVD method; **b,c**, Raman (**b**) and PL (**c**) spectra of the corresponding MoS<sub>2</sub> monolayer.



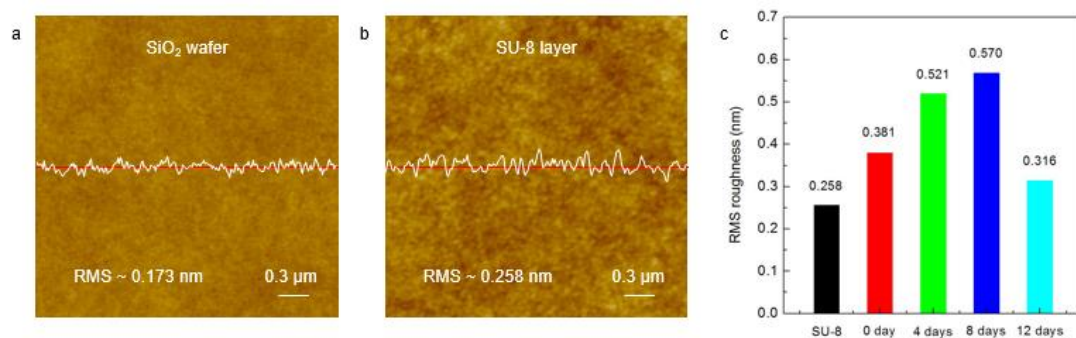
**Supplementary Figure 2 | SHG characterization of monolayer MoS<sub>2</sub> crystals with different dissolution time.** **a-c** SHG mapping images of MoS<sub>2</sub> crystals on SU-8/sapphire substrate kept in PBS solution at 75 °C within 0 day (**a**), 4 days (**b**) and 8 days (**c**).



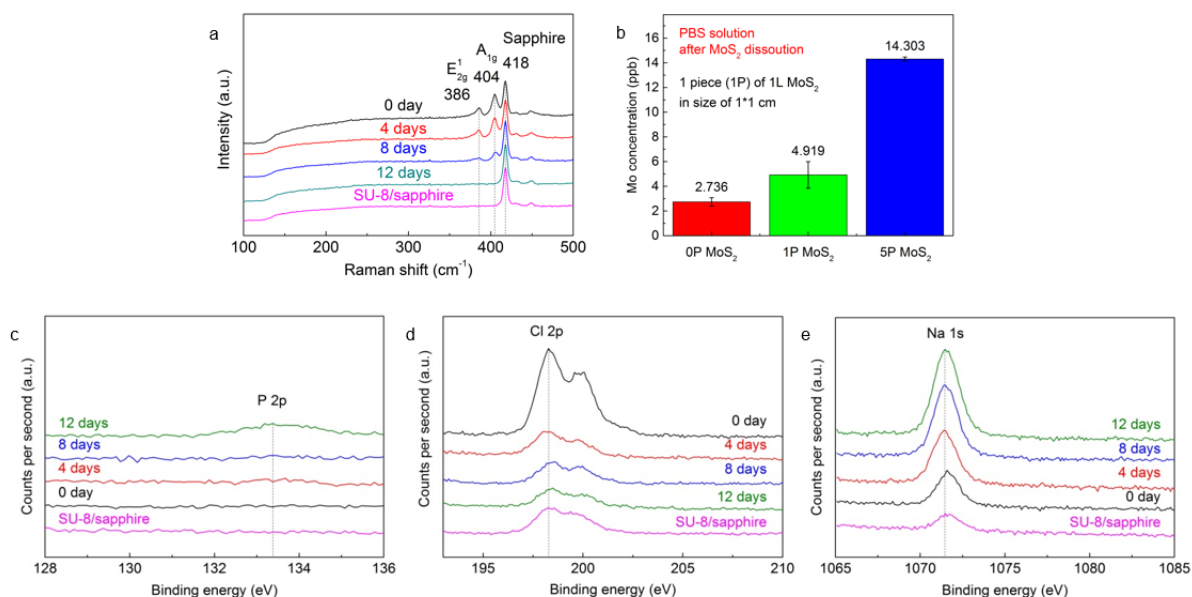
**Supplementary Figure 3 | Morphology evolution of monolayer MoS<sub>2</sub> crystals with different dissolution time.** a-c OM images of MoS<sub>2</sub> crystals on SU-8/sapphire substrate after kept in PBS solution at 75 °C for 21 (a), 35 (b) and 49 (c) days, respectively.



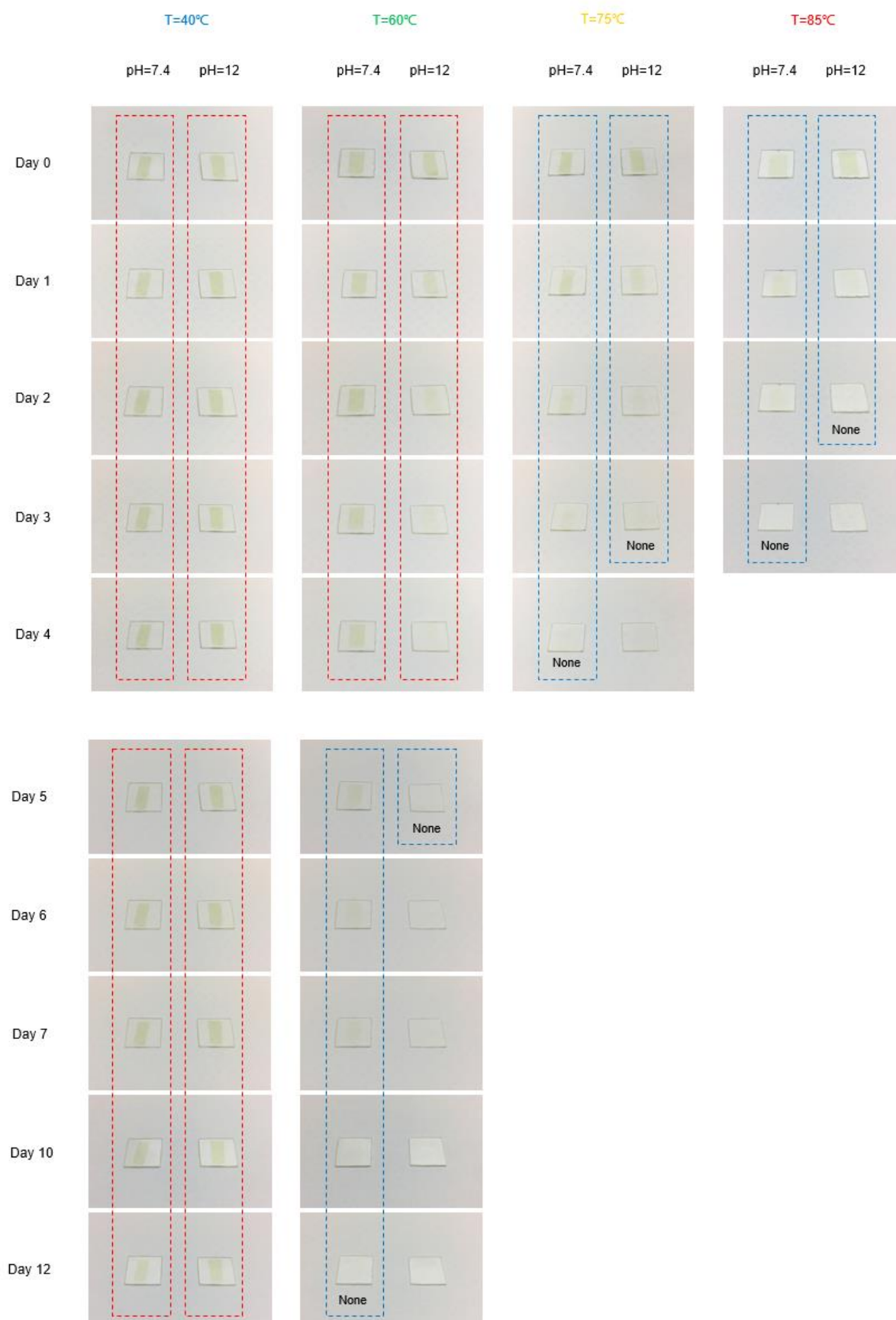
**Supplementary Figure 4 | Optical and structural characterization of monolayer MoS<sub>2</sub> continuous film.** a, OM image of monolayer MoS<sub>2</sub> continuous film on SiO<sub>2</sub> substrate synthesized by using LPCVD method; b, AFM images of the related MoS<sub>2</sub> film before and after oxidation to visualize its grain boundary; c-f Raman (c), PL (d) and XPS (e, f) spectra of the corresponding MoS<sub>2</sub> film.

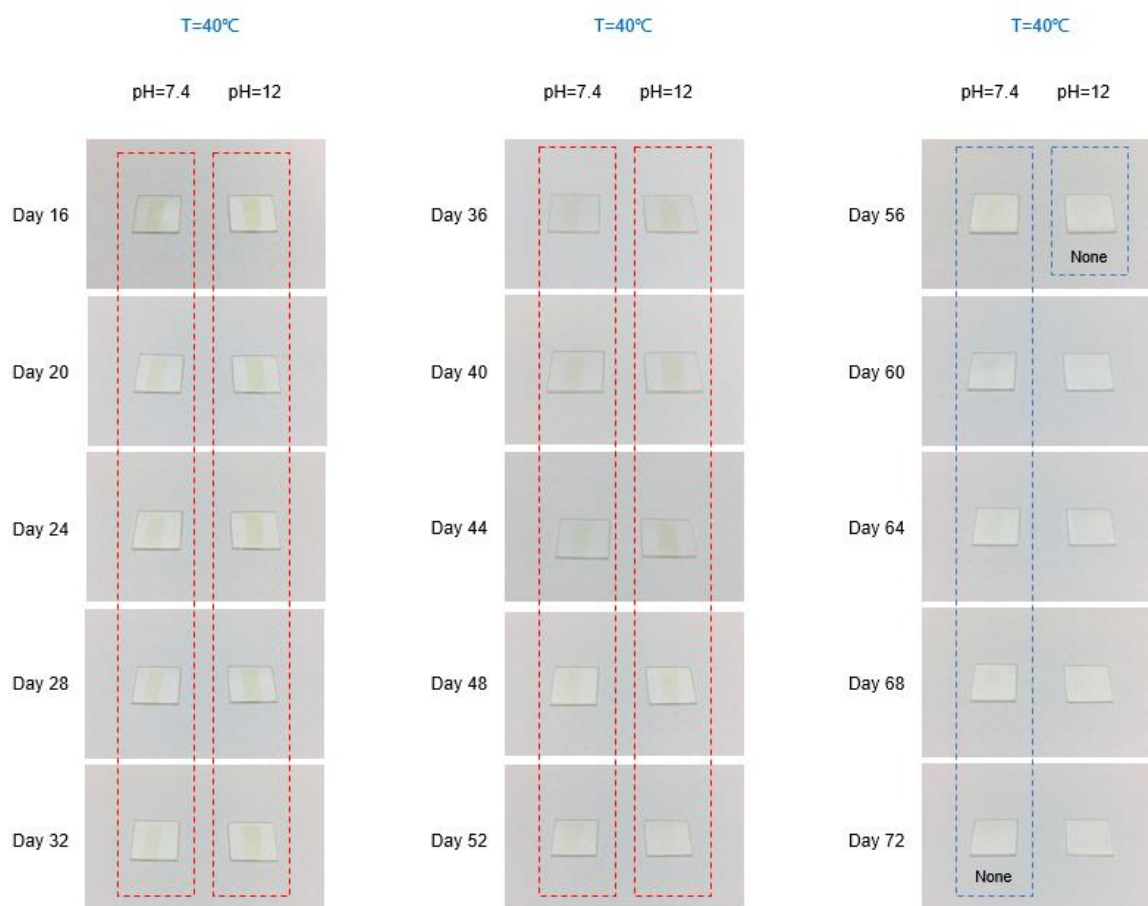


**Supplementary Figure 5 | Surface roughness of SU-8 layer and monolayer MoS<sub>2</sub> film with different dissolution time.** a,b, AFM images of SiO<sub>2</sub> (a) and SU-8 (b) substrates; c, RMS roughness evolution of SU-8 substrate and monolayer MoS<sub>2</sub> on SU-8 with different dissolution times from 0 day to 12 days in PBS solution at 60 °C.



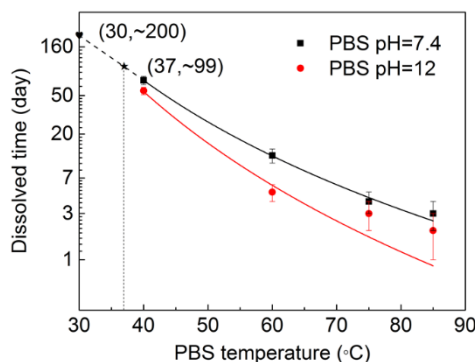
**Supplementary Figure 6 | Raman, ICP-MS, and XPS study of monolayer MoS<sub>2</sub> film with different dissolution time or PBS solution.** a, Time-dependent Raman spectra of the dissolved MoS<sub>2</sub> monolayers, with Raman shift ranging from 100 to 500 cm<sup>-1</sup>; b, Mo concentration in PBS solution before and after monolayer MoS<sub>2</sub> dissolution, measured by using inductively coupled plasma mass spectrometry (ICP-MS); c-e, XPS spectra of P (c), Cl (d) and Na (e) from the monolayer MoS<sub>2</sub> film on SU-8/sapphire with different dissolution time from 0 day to 12 days in PBS solution at 60 °C.



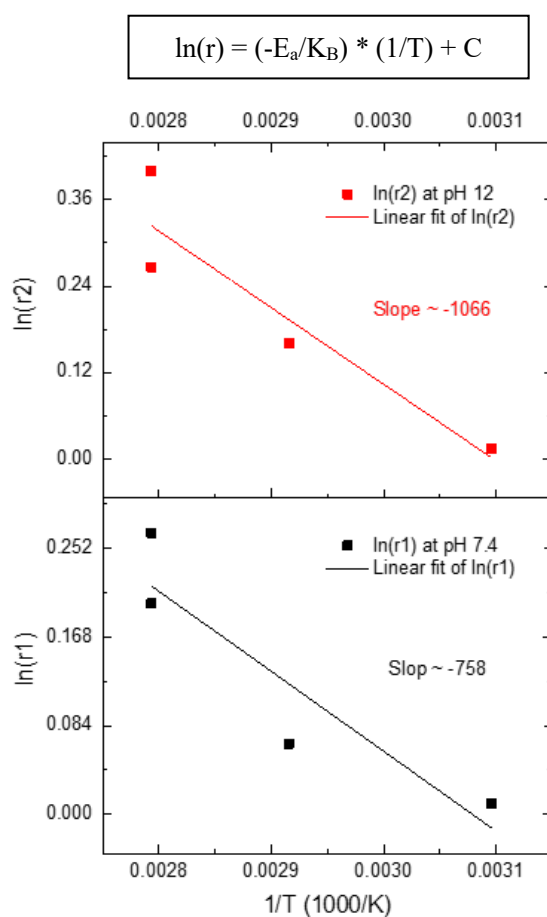


### Supplementary Figure 7 | Temperature-, pH- and time-dependent dissolution of monolayer MoS<sub>2</sub> film.

Optical images of large-scale MoS<sub>2</sub> monolayers on SU-8/sapphire substrate (1×1 cm) kept in PBS solution with different temperature (40-85 °C), pH level (7.4-12) and time (0-72 days). After 12 days, monolayer MoS<sub>2</sub> films in PBS solution at 60, 75 and 85 °C were all degraded except the one at 40 °C. Since then, we observed the samples at 40 °C until the end (72 days).

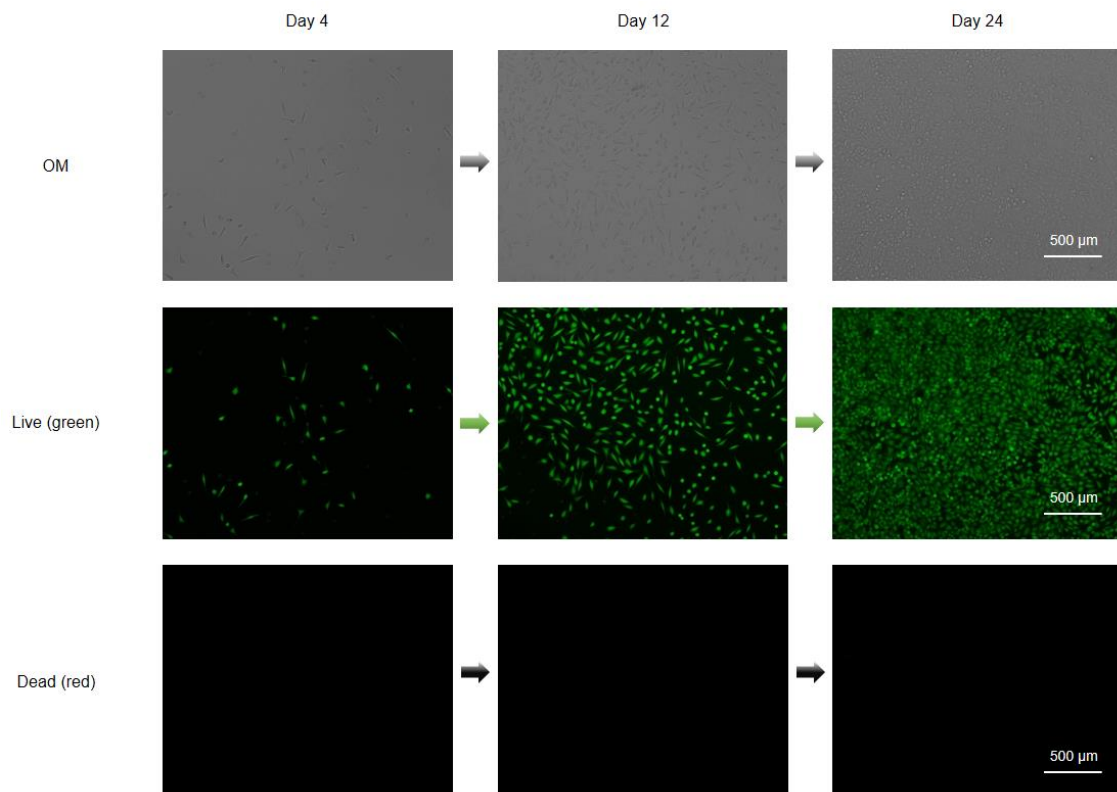


**Supplementary Figure 8 | Temperature- and pH-dependent speed at which the MoS<sub>2</sub> monolayer dissolved in PBS solution.** The linear scale of y axis has been converted into ln scale. Error bars of the experimental data represent standard error of mean.

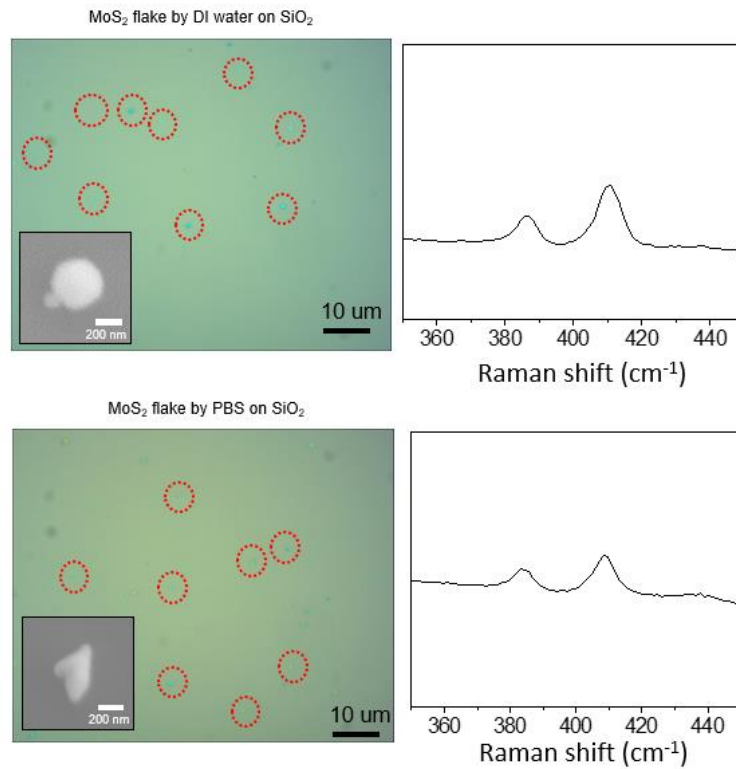


**Supplementary Figure 9 | Temperature- and pH-dependent dissolution rate of monolayer MoS<sub>2</sub> film.** Plots of the natural logarithm of the monolayer MoS<sub>2</sub> dissolution rates (r) as a function of the inverse of the temperature (T) at pH 7.4 and 12. The slope of the linear fitting estimates the activation energy as shown in the equation (Top of the figure). The equation was derived from the previous reported research (Ref. 14 in main text).

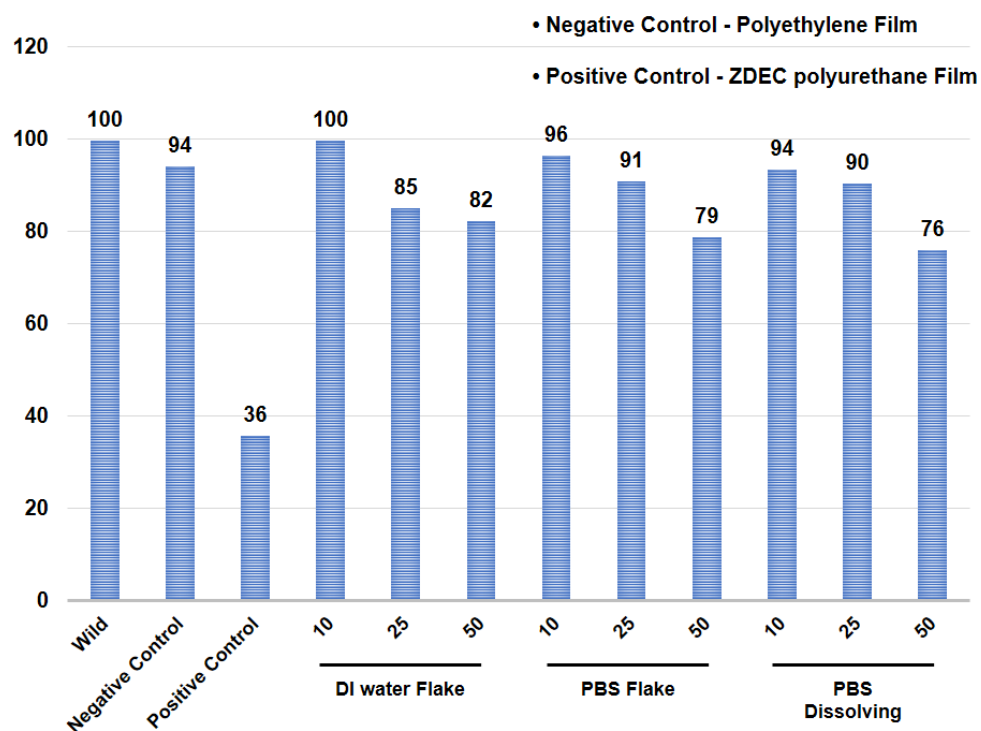




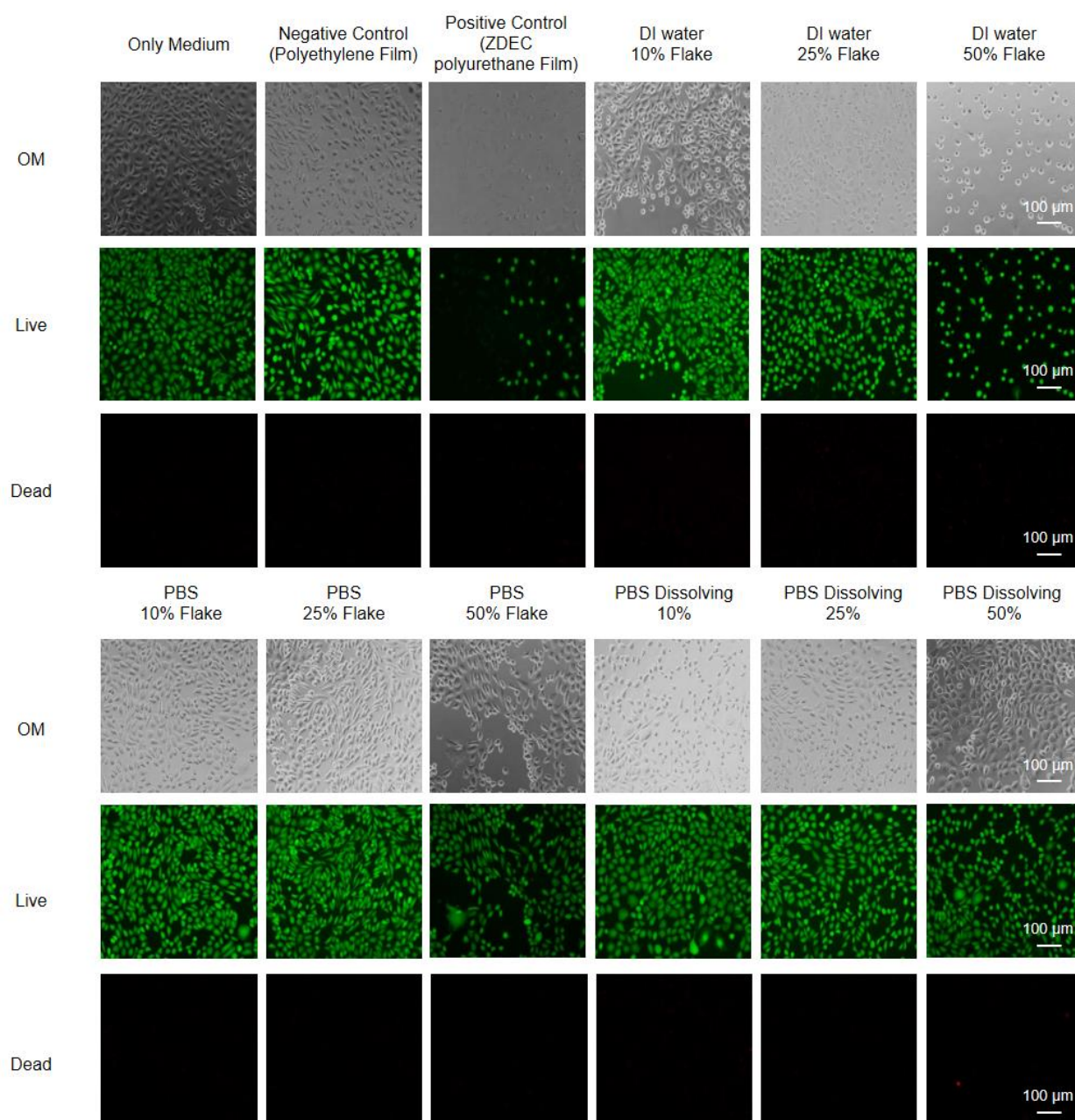
**Supplementary Figure 10 | Time-dependent cell culture on monolayer MoS<sub>2</sub> film.** OM and fluorescent images of cell culturing on monolayer MoS<sub>2</sub> film for 4, 12 and 24 days.



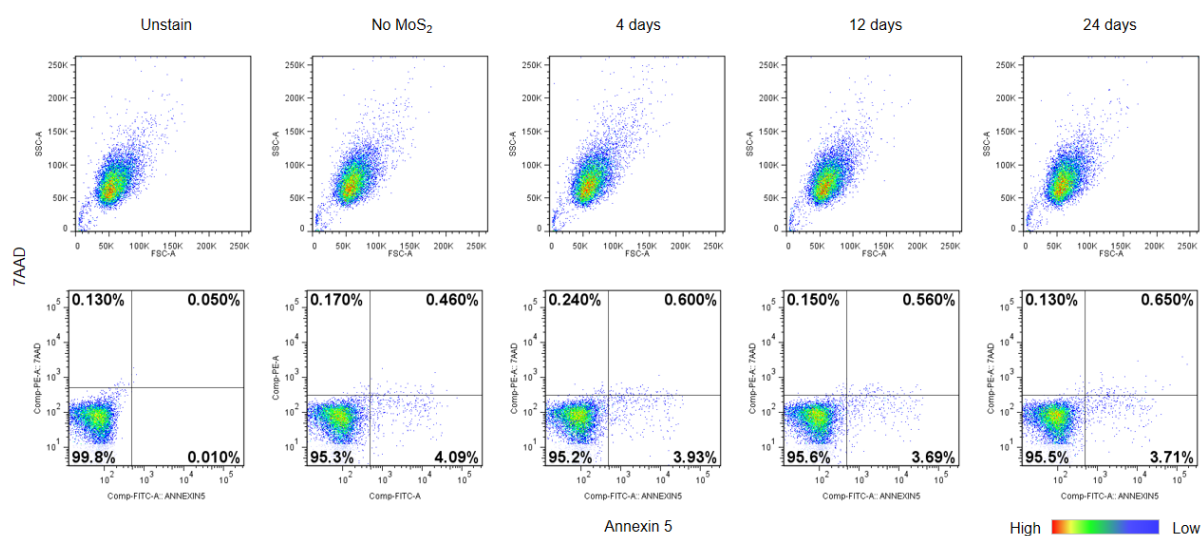
**Supplementary Figure 11 | Morphological and structural characterization of MoS<sub>2</sub> flake obtained from the continuous film.** OM images of dispersed MoS<sub>2</sub> flake in DI water and PBS solution and corresponding Raman spectra on SiO<sub>2</sub> substrate. Insets are the SEM image of the MoS<sub>2</sub> flakes in size of 300~400 nm.



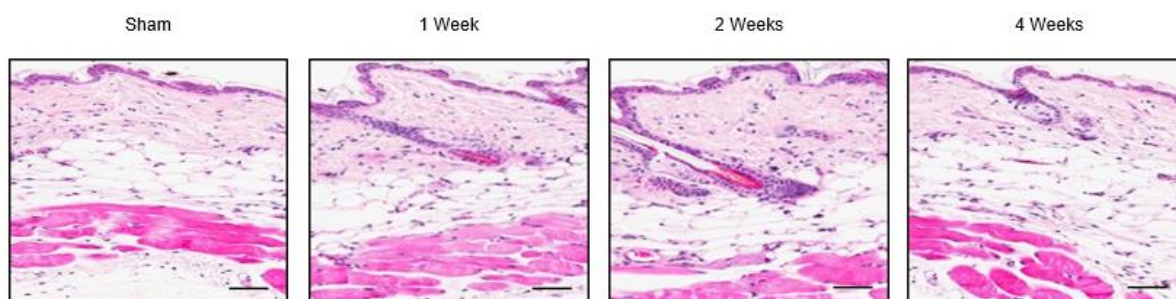
**Supplementary Figure 12 | The statistical results of cell viability.** Cell viability of L-929 cells on MoS<sub>2</sub> flake in DI water and PBS solution, dissolved MoS<sub>2</sub> in PBS, Culture medium, HDPE and ZDEC by CCK-8 assay.



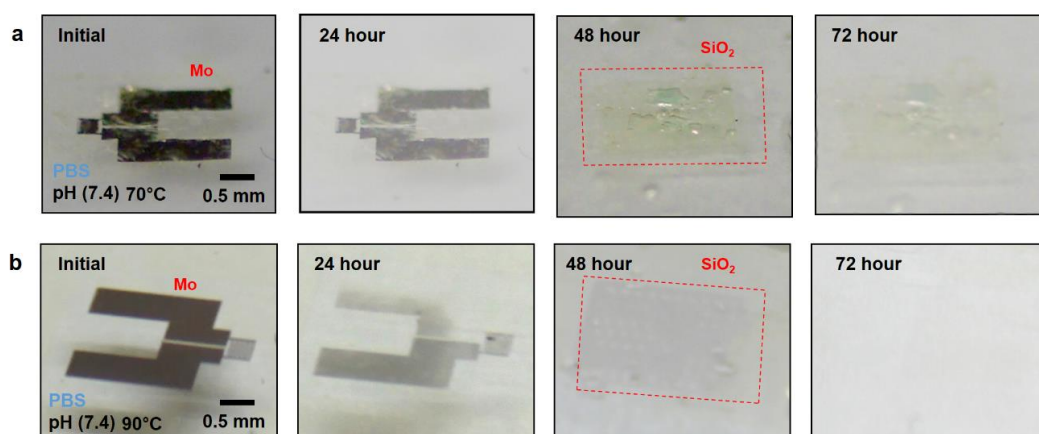
**Supplementary Figure 13 | Cell culture results in different mediums.** Set of differential interference contrast images and fluorescent images showing the cell viability of culture medium, HDPE, ZDEC, MoS<sub>2</sub> flake in DI water (10%, 25%, 50%), MoS<sub>2</sub> flake in PBS (10%, 25%, 50%), and dissolved MoS<sub>2</sub> in PBS (10%, 25%, 50%).



**Supplementary Figure 14 | Apoptotic population study based on 2D MoS<sub>2</sub> film.** Estimation of apoptotic populations in L929 of culture on MoS<sub>2</sub> film over 24 days using by Annexin V and 7-AAD, stained using flow cytometry.



**Supplementary Figure 15 | *In vivo* biocompatibility studies.** Representative microscope images (scale bar: 100 μm) of hematoxylin and eosin (H&E) stained tissue sections after 0-4 weeks post-implantation.



**Supplementary Figure 16 | Time-dependent dissolution process of the 2D MoS<sub>2</sub> bioabsorbable device.** Dissolution images collected at 4 stages of the accelerated condition of a system immersed in an aqueous buffer solution (pH 7.4) at 70 °C (a) and 90 °C (b).

### Supplementary References:

1. Wang, X., Shen, X., Wang, Z., Yu, R. & Chen, L. Atomic-scale clarification of structural transition of MoS<sub>2</sub> upon sodium intercalation. *ACS nano* **8**, 11394-11400 (2014).
2. Zhang, L. *et al.* In situ TEM observing structural transitions of MoS<sub>2</sub> upon sodium insertion and extraction. *RSC Adv.* **6**, 96035-96038 (2016).
3. Wang, Z. *et al.* Chemical Dissolution Pathways of MoS<sub>2</sub> Nanosheets in Biological and Environmental Media. *Environ. Sci. Technol.* **50**, 7208-7217 (2016).